Stabilized platinum electrodes for ferroelectric film deposition using Ti, Ta and Zr adhesion layers

T. Maeder, L. Sagalowicz, and P. Muralt

Laboratoire de Céramique, Ecole Polytechnique Fédérale de Lausanne, CH-1015 Lausanne, Switzerland.

Version of record: Japanese Journal of Applied Physics 37 (4A), 2007-2012, 1998.
©1998 The Japan Society of Applied Physics
http://hdl.handle.net/10.1143/JJAP.37.2007

Abstract

Pt-based metallizations using different adhesion layers (Ti, Zr and Ta) were studied for use as electrodes for ferroelectric thin films on oxidized silicon substrates. Different ways of oxidizing the adhesion layers prior to ferroelectric film growth are compared, with regard to obtaining stable, adherent Pt films of well-defined (111) orientation, while avoiding lead diffusion through the electrode. Upon in-situ deposition of $PbTiO_3$ at high excess lead flux, lead diffusion through the Pt film was found to depend strongly on the adhesion layer and the stabilization treatment. Pre-oxidation reduces lead diffusion during the later processing. Ti diffuses through the electrode for oxidation reaction, whereas Ta and Zr stay in place, in analogy to the diffusivities in the corresponding oxides. A novel oxidation treatment was developed to produce stable, adherent metallizations with controlled orientation and good barrier properties against lead diffusion.

***Keywords**: ferroelectric thin films, integration, adhesion layer, thermal stabilization*

1 Introduction

The recent development of ferroelectric thin films of the $Pb(Zr,Ti)O_3$ (PZT) family for memory [1], piezoelectric [2] and pyroelectric [3, 4] devices has drawn considerable interest to integration issues. The prime concern is bottom electrode stability against the conditions prevailing during PZT film in-situ growth or crystallization annealing: oxidizing ambients and the presence of lead oxide at high temperatures (550-700°C). Degradation of the bottom electrode structure may affect adhesion, PZT properties and electrode conductivity and morphology [5-7], whereas lead oxide can diffuse through Pt and react with SiO_2 to form silicates[5, 7] or compounds with the adhesion layers.

Most metallizations on Si-SiO_2 use an adhesion layer, usually Ti, as its absence has been found to lead to poor adhesion [8]. Problems with diffusion and oxidation of Ti above and below Pt occur [6, 9-12]. TiO_2-Pt metallisations have shown far superior stability [10]. On the other hand, some diffusion of Ti into the Pt grain boundaries has been shown to enhance PZT nucleation, due to the probable creation of nucleation sites, compared to the stable TiO_2-Pt metallisations[13]. Annealing of the bottom electrode (Ti-Pt) prior to PZT deposition has been used [8] to achieve both stabilization and nucleation site creation. Diffusion of Ti into PZT is rather beneficial, for Ti is part of PZT and facilitates its nucleation of the perovskite phase by locally shifting the PZT composition towards the more easy to crystallize $PbTiO_3$ [14]. In case of Ta-Pt, too much Ta diffusion into PZT may lead to pyrochlore ($Pb_2Ta_2O_7$) formation, since the Ta^{5+} ion has the wrong valence for the B-site of the perovskite lattice. There is, however, a need for the use of Ta. In applications involving micromachining of Si wafers, Si_3N_4 is often used above or instead of SiO_2. On Si_3N_4, Ta is preferable to Ti, due to adhesion problems of the latter [2].

Overall, although various adhesion layers and stabilization treatments have been studied, no systematic comparison regarding diffusion mechanisms has been carried out. In this paper, we compare Ti, Zr and Ta with and without in-situ oxidation treatments with respect to adhesion layer composition, lead diffusion through and into Pt, and platinum film texture. These three metals are reactive to oxygen and hence well suited for adhesion layer applications. Differences are expected as concerns diffusion behavior and reaction with PbO. The goal of the present work is to determine the various diffusion and reaction mechanisms going on during processing, and to find suitable stabilization procedures.

2 Experimental

The metallizations have been DC magnetron sputter-deposited in one run at 400°C (+/-20 °C) in a Nordiko 2000 chamber. Four different processing schemes (see fig. 1) have been pursued in order to evaluate the stabilization effect of oxidation treatments at different stages of the electrode fabrication. The first type (Fig. 1A) is the basic, unstabilized metallisations, with typically 10 nm of adhesion layer and 80 nm Pt, serving as reference. In addition to the earlier proposed post-deposition anneal in oxygen (fig. 1B), or the anneal of the adhesion layer in oxygen (fig. 1D), we used a novel stabilization scheme with and intermediate oxidation step, as depicted in fig. 1C. This method aims at maintaining the well textured growth of platinum as obtained with types A and B, while avoiding nucleation of platinum on oxides as in type D, which results in an inferior texture quality. By oxidizing the adhesion layer before all the Pt has been put down, diffusion of adhesion layer metals along the grain boundaries of platinum to the top of the platinum surface is intended to be blocked.

The details of the type C metallization are as follows: After deposition of 35 nm of platinum the metallisations is in-situ oxidized during 10 minutes in the sputtering chamber, at 620°C in 10.5 Pa O_2. Afterwards, the temperature is lowered back to 400 °C and the remainder (50 nm) of the Pt is deposited.

In the case of Pt/Ta two more studies were done, namely (1) the effect of oxidation temperature on interdiffusion in case of the intermediate oxidation, and (2) the comparison of intermediate oxidation (type C) vs. post-oxidation (type D).

The crystalline orientation of the polycrystalline platinum film has been determined by X-ray diffraction (XRD), using two criteria: 1) texturation indices [15] of (111), (200) and (311) Pt peaks, and 2) rocking curve full width at half maximum (FWHM) of the Pt (222) peak. The resistance to lead diffusion of the metallisations was evaluated by the deposition of a 300 nm thick $PbTiO_3$ film at high excess lead flux (PbO flux : TiO_2 flux = 2) and high temperature (570°C). The $PbTiO_3$ deposition process by *in-situ* reactive sputtering, which took about 100 min, is described elsewhere [16, 17]. Cross-sectional transmission electron microscopy (TEM) was used to examine the samples. Pt orientation and $PbTiO_3$ crystallization was assessed by X-Ray diffraction (XRD).

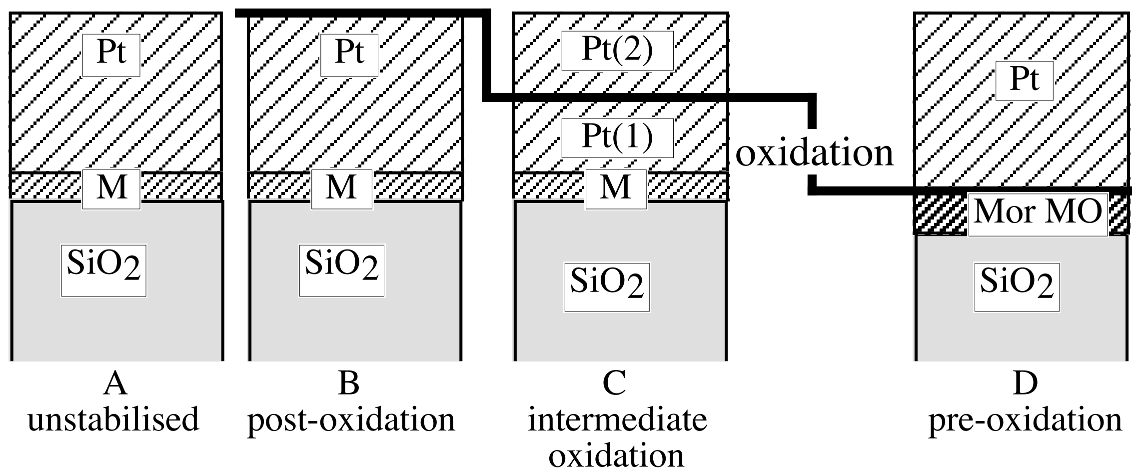

Figure 1. The four metallization types, where type A is the basic, unstabilized metallization and types B to D differ by where the oxidation treatment takes place. M stands for Ti, Zr or Ta, MO for their oxide in the as-deposited state.

For Pt/Ta metallizations, XRD was also used to quantify lead-tantalum interdiffusion, as the diffusion product, namely the pyrochlore phase, shows up easily on the spectra. The intensity of the (222) peak of the cubic pyrochlore structure ($d = 302$ to 309 pm) was used for this purpose. Also, the position of this peak was used to get a rough estimate of the Pb/Ta ratio (see Appendix).

3 Results

It was found that the growth of (111)-textured platinum on oxidized adhesion layers (type D treatment) is much more difficult to achieve. Moreover, adhesion is worse than with metallic adhesion layers. It was impossible to process Ta_2O_5-Pt films in developer solutions for standard photolithography [2]. The effect of post annealing (stabilization of type B) of Ti-Pt is already treated in a number of papers [5, 10]. The diffusion phenomena of this treatment are, of course, the same as during the heat treatment of the first part of the platinum film in case of the intermediate anneal (type C). We thus concentrate on reporting the results of the novel type C treatment, taking the standard non-annealed electrodes (type A) as reference for comparison. But we will also briefly compare type B treatments with respect to the others.

All Pt metallizations were smooth and featureless as deposited. The texturation indices (P_{111}, P_{200} and P_{311}) and Pt (222) rocking curve FWHM values ($\Delta\alpha$) are given in Table I. Complete (111) orientation of Pt and low FWHM is found for all samples of type A and C. Only in the Ti-Pt system, a slight degradation of orientation occurs by the intermediate anneal. The orientation is, however, still much better than in case of Pt/TiO_2 (type D). The extra Ta-Pt samples also show complete (111) orientation.

The diffusion behavior of all 6 samples after deposition of the $PbTiO_3$ layer, as seen from TEM, is schematically drawn in Fig. 2, and summarized in Table II. Selected TEM micrographs are shown in Figs. 3-5.

3.1 Ti-Pt

The most widely applied metallization, Ti-Pt, is also the most unstable, as seen from Fig. 3a. PbO diffuses very easily through the oxidized Ti layer into the SiO_2, as revealed by the contrast on the micrograph. The remaining thickness of TiO_x under Pt is very thin (<10 nm), compared to 20 to 25 nm expected for complete oxidation of the Ti layer. The major part of the adhesion layer has hence out-diffused into the Pt grain boundaries or the PbTiO3, in agreement with previously reported results [6, 8, 10-12]. Most probably, the remaining TiO_2 adhesion layer is porous, as is reported for the oxidation of bulk titanium [18].

Electron energy loss spectroscopy (EELS) analysis confirms that the Ti is oxidized. TiO_x (assumed to be TiO_2) precipitates are seen in the Pt (fig. 3b). Strangely, no PbO is found, neither in these precipitates nor in the Pt, although a considerable amount has passed through the metallisations into the SiO_2. Sometimes, traces of Pb are found at the Pt/Ti interface by energy dispersive spectroscopy (EDS). Such a behavior can be explained as follows: The TiO_2 precipitates open the grain boundaries between platinum grains. Along these open grain boundaries PbO diffuses as quickly as on the surface. The columnar microstructure of platinum, together with the porosity of the titania adhesion layer are favorable for a fast Pb diffusion into SiO_2. The diffusion is not homogeneous, but follows certain paths defined by the platinum grain structure. For this reason, no residual Pb is detected in the platinum and only a few traces are revealed in the adhesion layer.

The up-diffusion of Ti is also well seen after the intermediate oxygen anneal (Fig. 3c) (type C). A strong contrast is observed between the Pt layers originating from strong TiO_x formation between the grains and on top of the first part of the platinum film, as determined by EDS. All the Ti being oxidized, no precipitates were evidenced in the second Pt layer. The strong out-diffusion of Ti accounts for the low (111) orientation of the stabilized Ti-Pt metallization. Obviously, the nucleation of the second Pt layer on the first is disturbed by the TiO_2 precipitates (Fig. 4). Lead diffusion into SiO_2 is still present. Again, PbO seems to interact little with TiO_2.

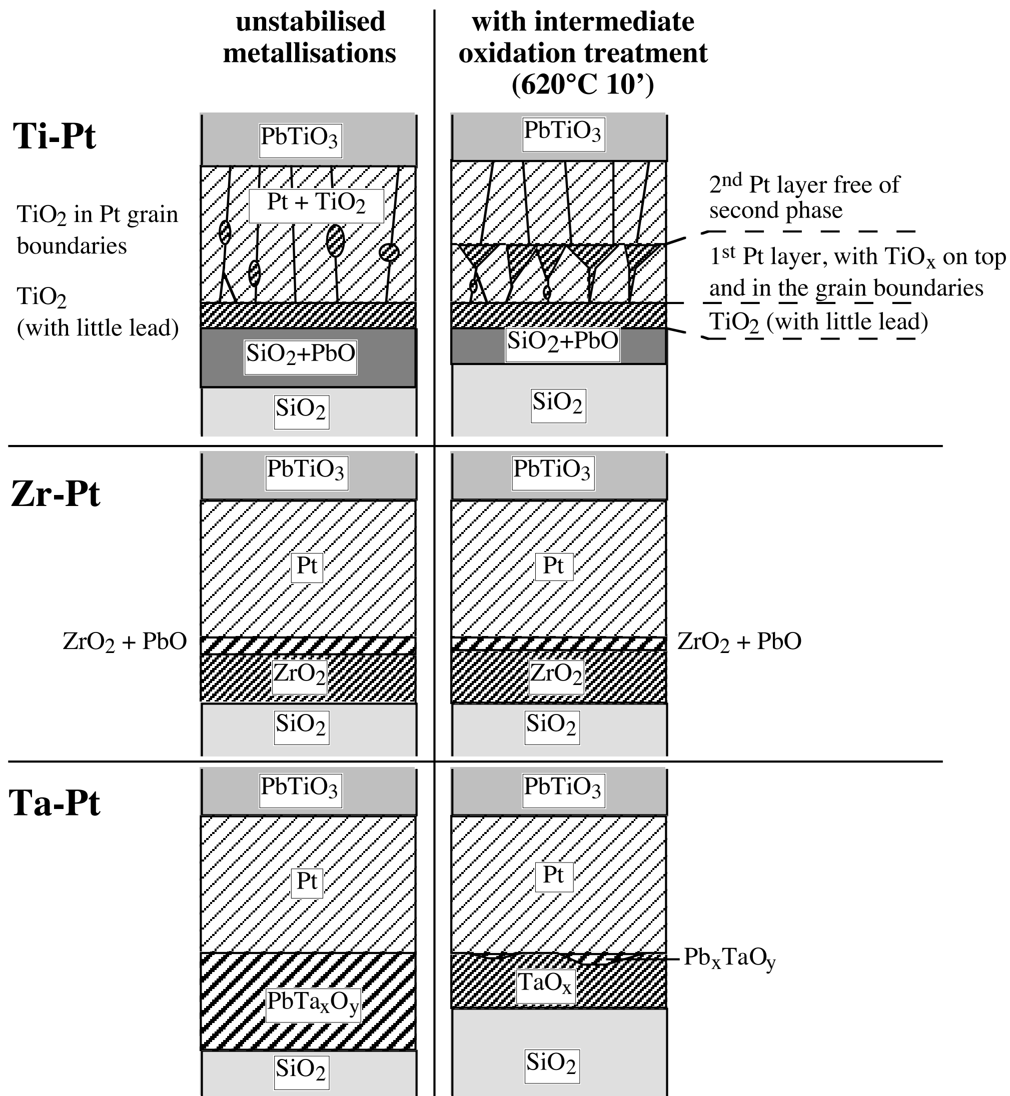

Figure 2. Schematised TEM observations, after $PbTiO_3$ deposition.

Table I. Texturation indices and Pt (222) rocking curve width vs. adhesion layer and stabilization treatment (intermediate oxidation).

Metallization	P_{111}	P_{200}	P_{311}	$\Delta\alpha$
Ti-Pt type A	3.00	0.00	0.00	2.9°
Ti-Pt type C	2.93	0.02	0.05	6.9°
Ti-Pt type D	2.05	0.07	0.88	19.1°
Zr-Pt type A	3.00	0.00	0.00	2.4°
Zr-Pt type C	3.00	0.00	0.00	1.9°
Ta-Pt type A	3.00	0.00	0.00	1.4°
Ta-Pt type C	3.00	0.00	0.00	3.1°

Table II. Summary of TEM observations, after $PbTiO_3$ deposition.

Metallization	Impurities in Pt	PbO diffusion into SiO_2	PbO in adhesion layer
Ti - Pt 12 - 85 nm type A	precipitates of TiO_x	heavy	present, but little reaction with TiO_2
Ti – Pt type C	TiO_2 in bottom Pt layer and between bottom and top layers, none in top Pt layer	medium	present, but little reaction with TiO_2
Zr - Pt 18 - 85 nm type A	none detected	none detected	slight reaction concentrated in top half of layer
Zr-Pt type C	none detected	none detected	slight reaction in top half of layer
Ta – Pt 10 - 85 nm type A	none detected	none detected	all layer transformed to lead tantalate
Ta-Pt type C	none detected	none detected	slight reaction

3.2 Zr-Pt

In the case of Zr, the results observed for the two types (fig. 2) are very similar. Zr oxidizes into a dense, continuous layer under Pt, and diffuses neither into the Pt nor to its surface in detectable amounts. The ZrO_x thickness is compatible with oxidation of all the Zr into ZrO_2. Opposite to Ti-Pt, no visible contrast is seen between the two Pt layers.

In both stabilized and unstabilized types, nanoprobe investigation reveal a slight lead diffusion, confined to the ZrO_2-Pt interface. No lead is detected in the SiO_2. The stabilization treatment has little influence in the case of Zr-Pt, although the PbO diffusion distance, if one compares the thickness of the reaction zone seen in the top part of the ZrO_2 layer, is lower (about 10 vs. 15 nm) in the stabilized case. The small observed difference can be accounted for by oxidation of the Zr in the preparatory stages of $PbTiO_3$ deposition. Indeed, Zr is the most reactive with oxygen of the three metals, an the easiest to fully oxidize.

3.3 Ta-Pt

Ta-Pt metallizations show a strong influence of stabilization treatments. In case the metallization was not oxidized prior to $PbTiO_3$ deposition, PbO diffusion is very strong, increasing by about 40% the thickness of the layer below the Pt (Fig. 5a) and giving a homogeneous, well-crystallized tantalate layer (Pb_xTaO_y). By EDS, it was measured that the atomic ratio Pb/Ta is about 0.5, which is compatible with the measured thickness increase. Although lead diffusion is very important and the Pb_xTaO_y is in contact with the SiO_2, no lead is seen in the latter. Chemical affinity between Ta_2O_5 and lead oxide therefore seems to be very strong.

In the stabilized case (type C), very little Pb (1%) is detected by EELS in TaO_x, corresponding likely to the observed precipitates (fig. 5b) near Pt, which form a few nm thick reaction layer. No PbO is observed in the SiO_2, and the TaO_x thickness is compatible with oxidation of all the Ta into Ta_2O_5, which is the stable oxide in our conditions. As in the case of Zr-Pt, Ta oxidizes essentially below Pt, forming a dense oxide layer.

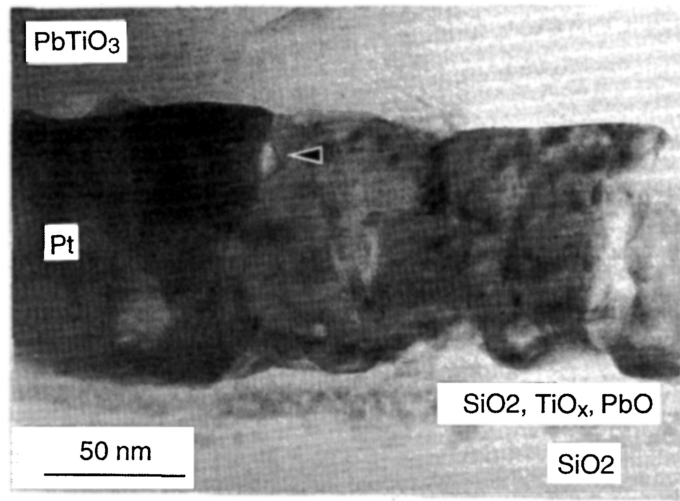

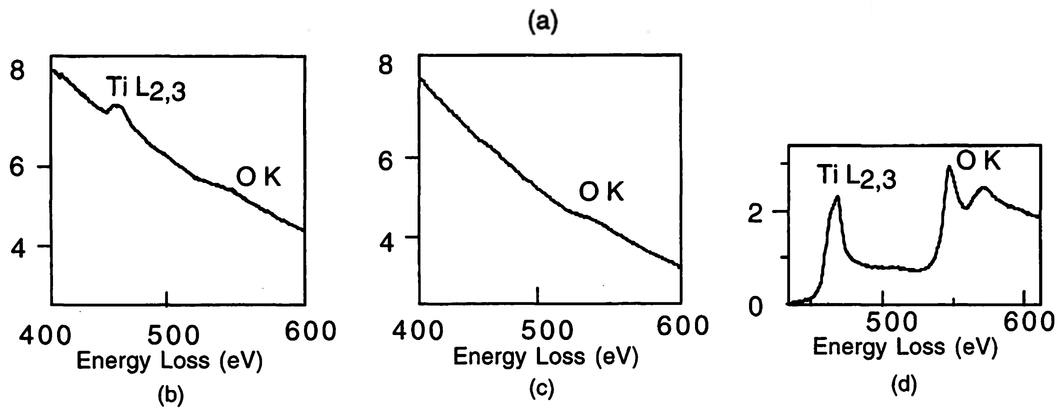

Figure 3. TEM micrograph of the unstabilized Pt/Ti electrode taken after $PbTiO_3$ deposition, showing a TiO_x precipitate (arrow) between two platinum grains; (b) EELS spectrum of the same precipitate proving that it contains Ti; (c) EELS spectrum from the interior of a platinum grain; (d) EELS spectrum from the adhesion layer.

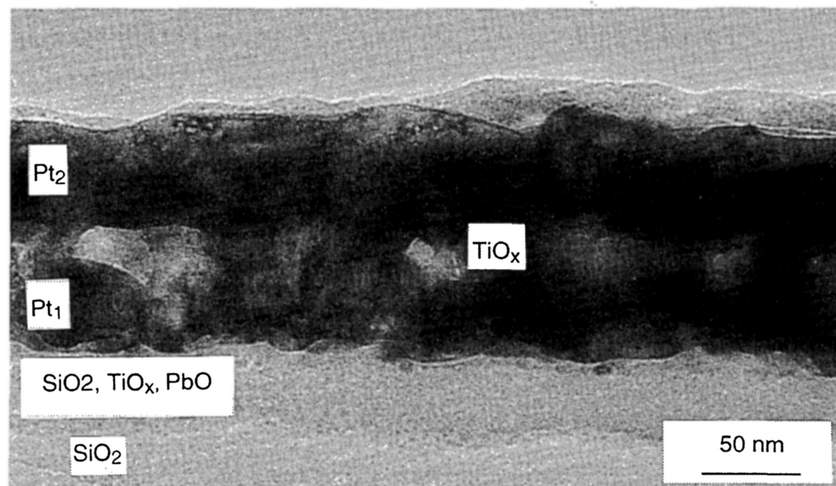

Figure 4. TEM micrograph of the stabilized Pt/Ti electrode (type C) taken after $PbTiO_3$ deposition. The chemical constituents of the layers are indicated as found by EELS.

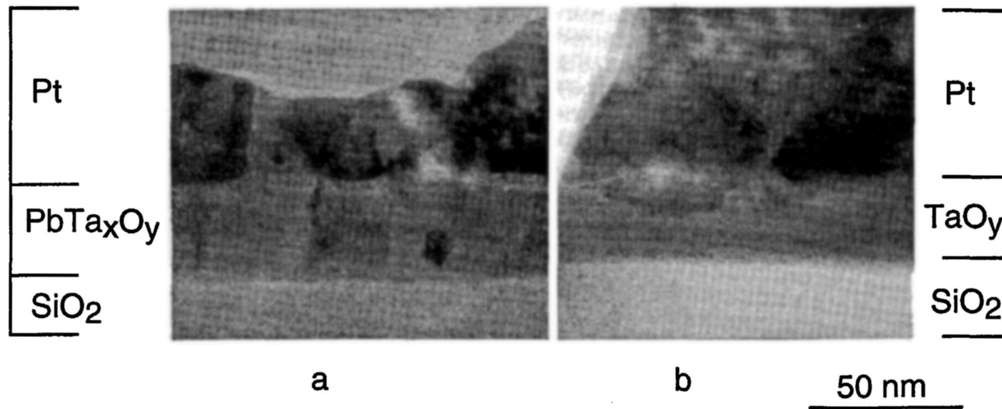

Figure 4. TEM micrograph of (a) the unstabilized Pt/Ta electrode, and (b) the stabilized Pt/Ta electrode (type C) taken after $PbTiO_3$ deposition. The chemical constituents of the layers are indicated as found by EELS.

The case of Ta is especially interesting, because it oxidizes like Zr, into a dense oxide below Pt, but the oxide has a strong affinity for PbO, even more than TiO_2. The results clearly demonstrate the oxidation mechanism is the most important factor leading to good barrier properties against lead diffusion: dense oxide films obtained by in-diffusion of oxygen are clearly desired, and, therefore, Zr and Ta are superior to Ti in this respect.

The influence of the temperature for the intermediate anneal has been studied by means of XRD. The product $PbTa_2O_7$ of lead-tantalum-oxygen reaction yields an intense (222) Bragg peak even for very thin films, indicating that the (222) planes grow mostly parallel to the substrate plane. The shift of this peak allows to estimate the Pb/Ta ratio according to Table A·I in the appendix. The intensity of the peak is a measure for the density of crystalline pyrochlore present in the adhesion layer. The results are in Fig. 6. The pyrochlore formation and thus lead diffusion decreases monotonically with increasing oxidation temperature. The estimated Pb/Ta ratio in the crystalline pyrochlore parts remains essentially constant at 0.8, dropping only when the lead diffusion is very low. The so evaluated Pb content differs somewhat from the result of the EDS analysis performed with 620° annealed samples. This is explained as follows: the X-ray signal is collected from the pyrochlore phase only, whereas the ED signal results from an average composition of the adhesion layer. In the annealed samples (type B) the transformation into pyrochlore is, however, not uniform throughout the adhesion layer, as in the case of type C treatments (Fig. 5b).

For comparison, post-oxidation of the metallization at 620°C (type B) was also assessed by XRD measurements. Two different anneal times of 10 and 60 minutes have been chosen. The results depicted in Fig. 7 show that post-oxidation is clearly beneficial compared to the unoxidised metallisations (type A), but is inferior to intermediate oxidation (type C). This is most probably due to the pollution of the Pt grain boundaries by Ta. Indeed, complementary X-ray Photo-Electron Spectroscopy (XPS) on as-deposited Ta-Pt metallizations reveal the presence of some Ta on the Pt surface. Nothing was detected, however, by means of electron spectroscopy (AES) measurements. This restricts the presence of Ta to the surface grain boundaries. This residual contamination is avoided by oxidizing the Ta, then depositing a layer of "fresh" Pt, as is done in type C.

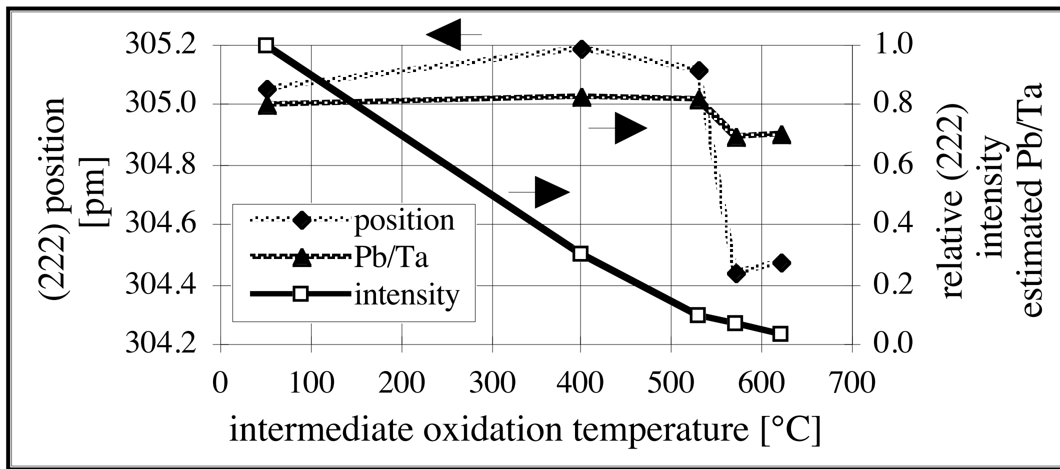

Figure 6. Intensity (relative to unoxidised Ta-Pt) of lead tantalate (222) peak, position and estimated Pb/Ta ratio vs. stabilization temperature.

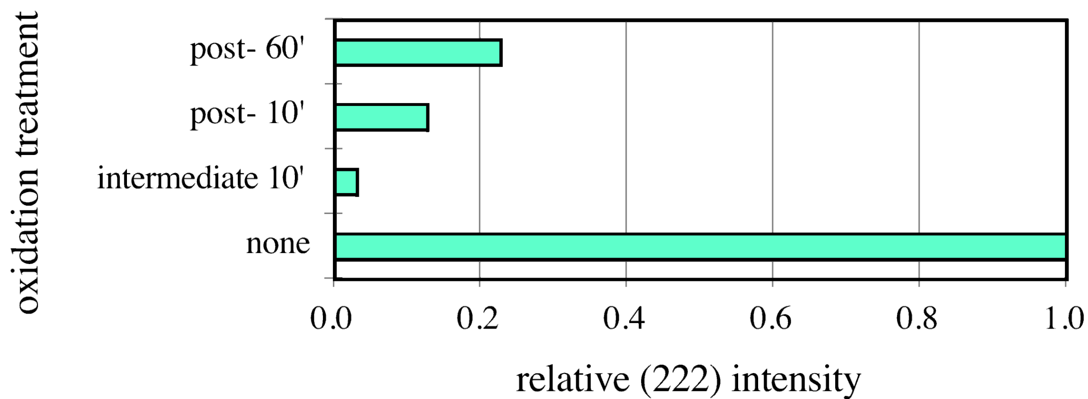

Figure 6. Intensity (relative to unoxidised Ta-Pt) of lead tantalate (222) peak, vs. stabilization type.

Table III. Oxides of Ti, Zr and Ta, Gibbs free energy of formation per mole of O_2, dominant diffusing species and compound formed with PbO [20-23].

Oxide	**Gibbs free energy of formation** $-\Delta G_f^0$ **[kJ/mol O_2]**	**Dominant diffusing species**	**Compound formed with PbO**
TiO_2	-888	Ti	$PbTiO_3$, perovskite
ZrO_2	-1036	O	$PbZrO_3$, perovskite
Ta_2O_5	-764	O	many compounds, often pyrochlore-type
PbO	-380	O	

4 Discussion

The experiments show that Pt alone is not a barrier against lead diffusion. The oxidation of the adhesion layer plays an essential role in this respect. The chosen adhesion metals clearly differ in their oxidation behavior. Whereas Zr and Ta form dense oxide layers below the platinum during oxygen anneals, Ti diffuses through the platinum film and forms oxide precipitates in grain boundaries inside the film or near to the surface. This behavior is compatible with the diffusion mechanisms in the corresponding oxides (see Table III). The diffusing species are oxygen in Ta_2O_5 and ZrO_2, and Ti in TiO_2. At the very beginning of the oxidation, all three metal species may diffuse upwards through grain boundaries. The down diffusion of oxygen must be more intense, however, and so the adhesion layer starts to get oxidized from top to bottom. This inhibits a further escape of Ta and Zr atoms. The oxidation of the corresponding layers continuous by oxygen diffusion through the oxide. In contrast, the Ti still may diffuse away through the forming oxide, leaving pores behind.

The metals also differ with respect to reaction with lead. Lead, oxygen and tantalum react easily to the pyrochlore compound $Pb_2Ta_2O_7$, whereas Pb-M-O ternary phases are not as easily formed in case of Zr and Ti. The corresponding activation energies seem to be too high. The diffusivity of lead is much lower in the dense zirconia than in the thinner and porous titania layer.

An important question concerns the timing of oxygen and lead diffusion. Does it matter whether they occur simultaneously or sequentially? At least in the case of Ta-Pt, lead diffusion is enhanced by simultaneous oxygen diffusion, for the lead content in post-annealed electrodes is lower than in untreated ones. One reason for this behavior might the be larger free energy of formation for the pyrochlore when starting from molecular oxygen instead from the oxide. Another reason might be due to reduction of PbO by tantalum (see Table III), thereby increasing the diffusivity of lead. This may happen by partial or complete oxidation of Ta, which is a strong exothermic reaction:

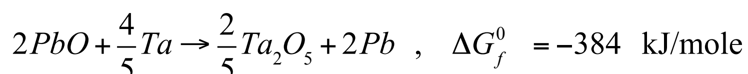

$$2PbO + \frac{4}{5}Ta \rightarrow \frac{2}{5}Ta_2O_5 + 2Pb \quad , \quad \Delta G_f^0 = -384 \text{ kJ/mole}$$

The other phenomena are well explained by the deterioration of the mechanical integrity of the platinum film by the oxidation reaction which precedes the lead diffusion. This is especially evident in the Ti-Pt system. The TiO_2 precipitates open the grain boundaries between platinum grains. Along these open grain boundaries PbO may diffuse as quickly as on a surface. The columnar microstructure of platinum, together with the porosity of the titania adhesion layer are favorable for a strong Pb diffusion into SiO_2. In the Ta and Zr systems much less oxide precipitates are observed, and so PbO diffusion is less rapid. With type C treatment, the role of the second half of the platinum layer is to re-establish the mechanical integrity of the platinum film after the anneal, i.e., to close the diffusion paths.

5 Conclusions

We have shown that the oxidation behavior of Ti, Zr and Ta adhesion layers can be predicted from the diffusion mechanisms of their respective oxides (TiO_2, ZrO_2 and Ta_2O_5). While Ti diffuses strongly into and through Pt upon oxidation, Zr and Ta essentially oxidize below Pt into a dense oxide layer. During $PbTiO_3$ film growth at high temperature and excess lead flux, the presence of unoxidised metallic adhesion layers below the Pt favors diffusion of PbO through the Pt grain boundaries. This diffusion is strongly reduced by oxidizing the Pt prior to $PbTiO_3$ deposition.

For Ta-Pt, it was shown that PbO diffusion decreases continuously with increase of the oxidation temperature (and hence the degree of oxidation). Also, carrying out the oxidation before the last Pt is put down, e.g. intermediate (type C) oxidation, allows to benefit from the nucleation of Pt on metals, while avoiding pollution of the Pt grain boundaries up to the metallisations surface, which is a problem of post-oxidation treatments (type B).

The oxidation behavior of Zr and Ta make them more suitable as adhesion layers than Ti. Their oxidation by oxygen in-diffusion benefit both stability (low lead diffusion) and orientation (undisturbed nucleation of second Pt layer). Zr is the most favorable, oxidizing faster and having lower reactivity with lead oxide.

Acknowledgement

This work was supported by the Swiss Priority Program on Materials (PPM) and the Swiss National Science Foundation.

References

[1] R.E. Jones, P. Zurcher, P. Chu, D.J. Taylor, Y.T. Lii, B. Jiang, P.D. Maniar, and S.J. Gillespie: Microelectronic Engineering **29** (1995) 3-10.

[2] P. Muralt, M. Kohli, T. Maeder, A. Kholkin, K.G. Brooks, and N. Setter: Sensors and Actuators A **48** (1995) 157-165.

[3] R. Takayama, Y. Tomita, K. Iijima, and I. Ueda: Ferroelectrics **118** (1991) 325-342.

[4] M. Kohli, C. Wüthrich, K. Brooks, B. Willing, M. Forster, P. Muralt, N. Setter, and P. Ryser: Sensors and Actuators A **60** (1997) 147-153.

[5] P.D. Hren, S.H. Rou, H.N.A. Shareef, M.S. Ameen, O. Auciello, and A.I. Kingon: Integrated Ferroelectrics **2** (1991) 311-325.

[6] R. Bruchhaus, D. Pitzer, O. Eibl, U. Scheithauer, and W. Hoesler: Materials Research Symposium Proceedings **243** (1992) 123-128.

[7] L.D. Madsen and L. Weaver: J. Electron. Mater. **21** (1992) 93-97.

[8] G.A.C.M. Spierings, J.v. Zon, M. Klee, and P.K. Larsen: Integrated Ferroelectrics **4** (1992) 283-286.

[9] G.A.C.M. Spierings, M.J.E. Uleneaers, G.L.M. Kampschöer, H.A.M.v. Hal, and P.K. Larsen: J. Appl. Phys. **70** (1991) 2290-2298.

[10] K. Sreenivas, I. Reaney, T. Maeder, N. Setter, C. Jagadish, and R.G. Elliman: J. Appl. Phys. **75** (1994) 232-239.

[11] G.R. Fox, S. Trolier-McKinstry, S.B. Krupanidhi, and L.M. Casas: J. Mater. Res. **10** (1995) 1508-1515.

[12] K.H. Park, C.Y. Kim, Y.W. Jeong, and H.J. Kwon: J. Mater. Res. **10** (1995) 1790-1794.

[13] R. Klissurska, T. Maeder, K.G. Brooks, and N. Setter: Microelectronic Engineering **29** (1995) 297-300.

[14] K.C. Chen and J.D. Mackenzie: Mat.Res.Symp.Proc. **180** (1990) 663-668.

[15] C.S. Barrett and T.B. Massalski, *Structure of metals, ,* R. Maxwell, Editor. 1980, Oxford: p. 204.

[16] T. Maeder and P. Muralt: MRS Symp. Proc. **341** (1994) 361-366.

[17] T. Maeder, P. Muralt, M. Kohli, A. Kholkin, and N. Setter: British Ceramic Proceedings **54** (1995) 207-218.

[18] N. Birks and G.H. Meier, *Oxidation of pure metals,* in *Introduction to high temperature oxidation of metals*. 1983, Edward Arnold: London. p. 66-90.

[19] *MacPDF (JCPDS Database)*. 1993, Helios Software: Norwich, USA.

[20] H. Matzke, *Diffusion in nonstoichiometric oxides,* in *Nonstoichiometric oxides,* O.T. Soerensen, Editor. 1981, Academic Press: New York. p. 155-232.

[21] J.E. Stroud and W.C. Tripp: J. Am. Ceram. Soc. **57** (1974) 172-175.

[22] R.C. Weast, ed. *Handbook of Chemistry and Physics*. 64th ed. 1984, CRC Press: Boca Raton, Florida.

[23] H.E. Brown: *Lead Oxide,* 1985, New York: Int. Lead Zinc Research Organization, Inc., p. 94.

Appendix: lead tantalates

PbO and Ta_2O_5 readily form lead tantalates. Many have a crystal structure derived from that of pyrochlore. Some possible products (from the JCPDS database [19]) are shown in Table A·I, with their Pb/Ta ratio and interplanar distance (d_{222}) of the (222) planes of the ideal cubic pyrochlore structure. The intensity of this (222) reflection was used to quantitatively assess the degree of interdiffusion. The quite regular increase of d_{222} with Pb/Ta ratio (see Fig. A·1) also allows a very rough estimate of Pb/Ta ratio from the peak position, which was calculated by linear regression according to the equation:

$$\frac{Pb}{Ta} \cong 0.176\left(d_{222}[pm]-300\right)-0.08$$

Table A·I. Pb/Ta ratio and (222) peak (cubic pyrochlore) interplanar distance (d_{222}) of some lead tantalates [19].

Pb/Ta	d_{222} [pm]	JCPDS No.
0.25	302	14-317
0.50	305	20-598
0.50	303	23-1165
0.67	304.4	36-1096
0.75	305	17-613
0.75	305	22-674
1.00	306	19-705
1.22	306.3	36-1096
1.25	306	19-704
1.40	309.1	36-1099
1.50	309	20-599
1.50	309	30-729
1.50	309	30-730

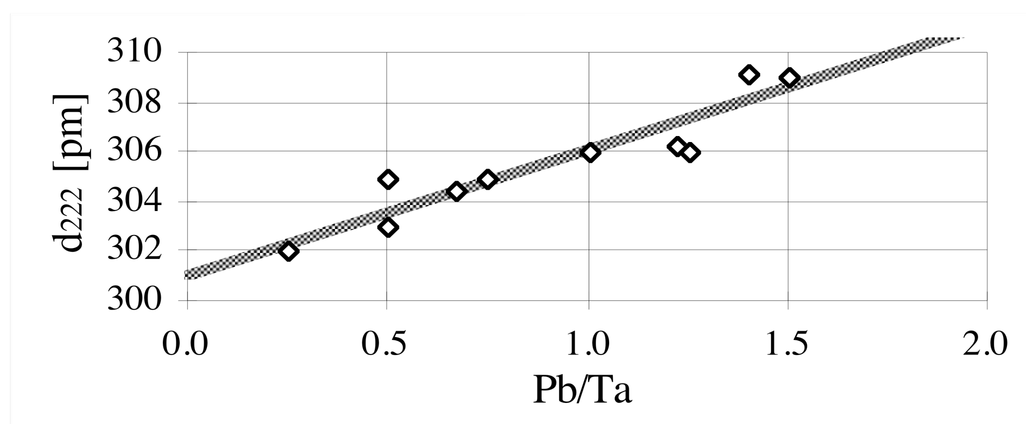

Figure A·1. Interplanar distance d_{222} vs. Pb/Ta ratio, with regression line, according to data in Table A·I.